Second-Order Phase Transition in Causal Dynamical Triangulations

Jan Ambjørn,[1,*] S. Jordan,[2,†] J. Jurkiewicz,[3,‡] and R. Loll[2,†]

[1]*The Niels Bohr Institute, Copenhagen University, Blegdamsvej 17, DK-2100 Copenhagen Ø, Denmark*
[2]*Institute for Theoretical Physics, Utrecht University, Leuvenlaan 4, NL-3584 CE Utrecht, The Netherlands*
[3]*Institute of Physics, Jagellonian University, Reymonta 4, PL 30-059 Krakow, Poland*

(Received 22 August 2011; published 15 November 2011)

Causal dynamical triangulations are a concrete attempt to define a nonperturbative path integral for quantum gravity. We present strong evidence that the lattice theory has a second-order phase transition line, which can potentially be used to define a continuum limit in the conventional sense of nongravitational lattice theories.

DOI: 10.1103/PhysRevLett.107.211303 PACS numbers: 04.60.Gw, 64.60.−i

Introduction.—Dynamical triangulations (DT) were invented as a nonperturbative regularization of bosonic string theory and thus also of two-dimensional quantum gravity coupled to conformal matter. This program was both a failure—in showing that even in a nonperturbative setting no bosonic string theory exists in dimension two or larger—and an amazing success, in providing a versatile regularization of 2D quantum gravity coupled to conformal matter with central charge $c \leq 1$, i.e., noncritical string theory. Surprisingly, in many ways the regularized theory turned out to be easier to solve analytically than the corresponding continuum theory.

Encouraged by this, DT was generalized to provide a regularization of quantum gravity in three [1–3] and four dimensions [4,5]. The naïve expectation was that if a ''stand-alone'' four-dimensional theory of quantum gravity existed, the regularized theory should have a second-order phase transition, which could be used to define a continuum theory of quantum gravity. Second-order transitions are usually characterized by a divergent correlation length associated with propagating field degree(s) of freedom, in the case at hand presumably of a gravitonic nature. If a given phase transition point was a UV fixed point, one could also attempt to make contact with Weinberg's asymptotic-safety scenario, for which plenty of corroborating evidence has been found recently (see [6] for reviews).

A phase transition point was indeed located in 4D DT, and at first believed to be of second order [4,7,8]. However, analyzing larger lattice systems changed the verdict to a first-order phase transition where no obvious continuum limit could be defined, at least not when using the Regge version of the Einstein-Hilbert action [9,10]. Neither did one find convincing evidence of a good classical behavior of large-scale geometry away from the phase transition.

Partly triggered by this impasse, a modified lattice model in terms of causal dynamical triangulations (CDT) was proposed, and subsequently shown to have long-distance properties in agreement with (semi-)classical gravity [11]. It still uses the Regge-Einstein-Hilbert action, but assumes the existence of a global time-foliation, and has a more complicated phase diagram than the simplest DT model. (The notable similarities with ''Hořava-Lifshitz gravity'' [12] are being explored, see e.g., [13].) In what follows, we will provide strong, new evidence that—unlike its Euclidean counterpart—4D CDT quantum gravity possesses a second-order phase transition line.

Causal dynamical triangulations.—We begin with a brief account of CDT, focusing on several important aspects (see [14–17] for technical details and [18] for reviews). CDT can be characterized as a nonperturbative path integral which is as close as possible to a canonical quantization: spacetime histories share a global foliation, where each leaf is a spatial hypersurface, given in terms of a three-dimensional triangulation of fixed topology $\mathcal{T}$, built from equilateral tetrahedra with link length a_s, and labeled by a discrete proper time t_n. Adjacent hypersurfaces are connected by four-simplices, resulting in spacetime histories of the form of four-dimensional triangulations of topology $\mathcal{T} \times [0, 1]$. We use $\mathcal{T} = S^3$ and impose periodic boundary conditions in time, such that the spacetime topology is $S^3 \times S^1$. The geometry of each spacetime is fixed by how the four-simplices are ''glued together'' to form a simplicial manifold, and by the lengths of its links, which come in two types: spacelike links which lie entirely within a given hypersurface, and timelike links whose end points lie on adjacent hypersurfaces, and which have a (squared) edge length $a_t^2 = \alpha a_s^2$, for some fixed relative scaling parameter $\alpha < 0$.

The CDT gravitational path integral is a sum over all geometrically inequivalent triangulations of this type with a fixed number of time steps, with amplitudes depending on the above-mentioned Regge-Einstein-Hilbert action [19]. Since in four dimensions analytical methods are mostly unavailable we use Monte Carlo simulations to extract physical results. To do this we must convert the path integral to a statistical partition function by applying a Wick rotation, which due to the foliated structure exists globally [15]. (The Wick-rotated geometries have Euclidean signature, as does their superposition, leading to

emergent geometries that likewise are of a Euclidean nature [11,14,16]. Their inverse Wick rotation will not be discussed in the present article.) It can be implemented by rotating $\alpha \to -\alpha$ in the lower-half complex plane, leading to the Euclidean Regge action

$$S_E = \frac{1}{G}\int \sqrt{g}(-R + 2\Lambda) \to -(\kappa_0 + 6\Delta)N_0 + \kappa_4 N_4 + \Delta(N_4 + N_4^{(4,1)}), \quad (1)$$

where N_0 and N_4 denote the total number of vertices and four-simplices and $N_4^{(4,1)}$ counts the subset of four-simplices which have four vertices on one hypersurface and the fifth on a neighboring one. The couplings κ_0, κ_4, and Δ are linearly related to the bare inverse gravitational coupling, the bare cosmological coupling, and the parameter α introduced above; Δ obeys $\Delta(\alpha = 1) = 0$ and increases when α decreases. Near the B-C transition shown in Fig. 1, α is close to 1.

Redefining $\tilde{\kappa}_4 = \kappa_4 + \Delta$, we obtain the Euclidean Regge action implemented in the computer simulations, namely,

$$S_{\text{Regge}} = -(\kappa_0 + 6\Delta)N_0 + \tilde{\kappa}_4 N_4 + \Delta N_4^{(4,1)} =: -\kappa_0 N_0 + \tilde{\kappa}_4 N_4 + \Delta\,\text{conj}(\Delta), \quad (2)$$

where for later convenience we have introduced the quantity $\text{conj}(\Delta) = N_4^{(4,1)} - 6N_0$ conjugate to Δ. This turns the gravitational path integral into a statistical partition function with Boltzmann weights $\exp(-S_{\text{Regge}})$. We will use the freedom to switch to a different ensemble, obtained by keeping N_4 (measuring the four-volume of the system) fixed, instead of its conjugate κ_4. In this way we can treat N_4 as a finite-size scaling parameter which does not appear in the phase diagram of the putative continuum theory. The remaining couplings κ_0 and Δ span the phase diagram, which we will go on to explore in the next section.

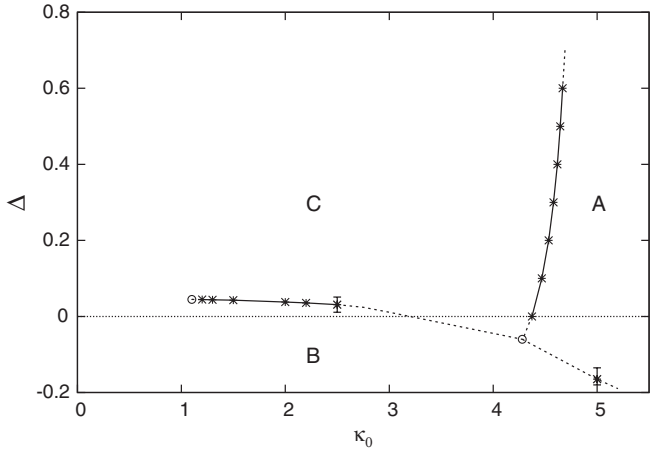

FIG. 1. The phase diagram of CDT. The large crosses represent actual measurements.

The phase diagram of CDT.—A qualitative description of the CDT phase diagram first appeared in [14], with a quantitative plot presented later in [13]. The diagram exhibits three phases, labeled A, B, and C in Fig. 1. A geometric characterization of the phases can be given in terms of their distinct spatial volume profiles $N_3(t)$, measuring the three-volume in lattice units as a function of proper time t. As described in detail elsewhere [16,17], the average large-scale geometry found in phase C shows the scaling behavior of a genuine four-dimensional universe. The average volume profile matches beautifully that of a Euclidean de Sitter spacetime. Even the quantum fluctuations around this emergent background geometry are described well by a cosmological minisuperspace action [17,20]. The situation in the other phases is completely different. The typical volume profile of a configuration in phase A shows an almost uncorrelated sequence of spatial slices, while the configurations in phase B are characterized by an almost vanishing time extension.

A preliminary analysis in [13] suggested that the A-C transition is of first order, similar in nature to the first-order transition observed in the DT formalism mentioned above. However, as also pointed out in [21], to nail down this result the numerical evidence still needs to be strengthened. By contrast, our interest in the present Letter is in the order of the B-C transition, about which considerable doubt remained in [13]. (Atypical for a first-order transition, the double-peak structure at the B-C line observed in [13] weakens with larger volume. Corresponding evidence that the transition is not first order can be quantified further [22]; the observables used below will show this even better.) We will present strong evidence below that it is a second-order transition line.

Before doing so, it is instructive to analyze how the transitions change as we move along the respective phase transition lines, while holding the system size fixed. The A-C transition line is characterized by a jump in N_0, the variable conjugate to the coupling constant κ_0, when we cross the line by changing κ_0. We see no appreciable change in this signal when we move along the A-C transition line, although we have not examined closely the triple point where all three phases meet.

The situation is very different for the B-C transition. When changing the coupling constant Δ and crossing the transition line, we observe a jump in the variable $\text{conj}(\Delta)$. However, moving to smaller values of κ_0 on the left, the jump decreases. Around $\kappa_0 = 1.0$, no signature of a phase transition remains. We conclude that the B-C transition has an end point, which for $N_4 = 80k$ is located around $\kappa_0 = 1.0$. Moving to the right the jump increases, and around $\kappa_0 = 2.3$ the transition is so strong that we get stuck in metastable states. The dashed part of the B-C line in Fig. 1 marks the region where conventional methods are insufficient to measure the location of the phase transition with acceptable accuracy. We are analyzing

currently whether the use of multicanonical Monte Carlo simulations can help in resolving this issue.

The order of the B-C phase transition.—Measuring the order of phase transitions requires some care. To confirm that a phase transition is not a first-, but a second-order transition, one can try to measure various so-called critical exponents. (To define the continuum limit associated with a second-order transition, one usually studies the correlation length of some observable of the theory, as advocated in the Introduction. To establish that there is such a transition in the first place, it is more efficient to study global properties of the partition function, and use the definition of the second-order transition as discontinuity of the second derivative of the free energy with respect to an appropriate coupling.) One such exponent measures the shift of a transition point with system size. Recall first how this works for a conventional system such as the Ising model with volume $V = L^d$, where d is the dimension of the system [23]. Considering the Ising model's temperature-driven phase transition and using the location of the maximum of the magnetic susceptibility to define a transition point $\beta^c(V)$, one finds the power-law behavior

$$|\beta^c(\infty) - \beta^c(V)| \propto V^{-1/\nu d} \tag{3}$$

for sufficiently large system sizes. The exponent ν governs the increase of the correlation length in a second-order transition as one moves towards the critical point $\beta^c(\infty)$ on an infinite lattice. For first-order transitions there is no correlation length and one expects a scaling like (3), with νd replaced by an exponent $\tilde{\nu}$ where $\tilde{\nu} = 1$ [24]. A sufficiently strong violation of $\tilde{\nu} = 1$ therefore signals the presence of a second-order transition. Another quantity of interest is the Binder cumulant

$$B_{\mathcal{O}} = \frac{1}{3}\left(1 - \frac{\langle \mathcal{O}^4 \rangle}{\langle \mathcal{O}^2 \rangle^2}\right) \tag{4}$$

associated with an observable $\mathcal{O}$ [24], which is always nonpositive and zero if the histogram of $\mathcal{O}$ is Gaussian. Evaluating $B_{\mathcal{O}}$ as a function of the couplings, its local minima lie at transition points. We can measure these minima for different system sizes and by extrapolation determine $B_{\mathcal{O}}^{\min}(1/N_4 = 0)$. At a second-order transition the histogram of $\mathcal{O}$ should converge to a single Gaussian distribution with the Binder cumulant going to zero. At a first-order transition it will go to a nonzero constant; however, its value at a weak first-order transition can be small.

To analyze the B-C transition, we fixed $\kappa_0 = 2.2$ and used systems of size 40, 50, 60, 80, 100, 120, 140, and $160k$. The number of sweeps used was approximately 2.5×10^6, with one sweep consisting of 1×10^6 attempted Monte Carlo moves. We have measured the shift exponent $\tilde{\nu}$ for the asymmetry parameter Δ using

$$\Delta^c(N_4) = \Delta^c(\infty) - C N_4^{-1/\tilde{\nu}}, \tag{5}$$

where C is a proportionality factor, and Δ^c has been defined using the location of the maximum of the susceptibility

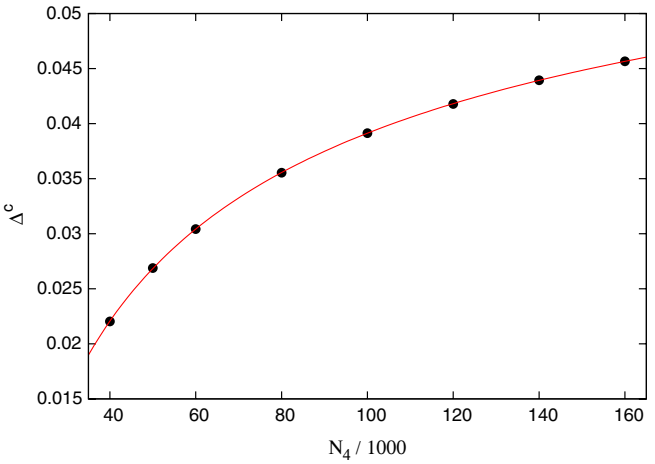

FIG. 2 (color online). Measuring the location Δ^c of B-C transition points at $\kappa_0 = 2.2$ for different system sizes N_4 to determine the shift exponent $\tilde{\nu}$.

$\chi_{\mathrm{conj}(\Delta)} = \langle \mathrm{conj}(\Delta)^2 \rangle - \langle \mathrm{conj}(\Delta) \rangle^2$. Figure 2 shows the measured data points (error bars too small to be included) and the best fit through all of them, yielding $\tilde{\nu} = 2.39(3)$. To judge whether our range of system sizes lies inside the scaling region we have performed a sequence of fits by successively removing the data points of lowest four-volume, leading to $\tilde{\nu}$ values 2.51(3), 2.49(3), and 2.51(5), where the last fit was performed with all but five data points removed. This suggests that the data point with the lowest four-volume lies outside the scaling region. Removing it from the fit we obtain

$$\tilde{\nu} = 2.51(3). \tag{6}$$

This result makes a strong case for a second-order transition, since the prediction $\tilde{\nu} = 1$ for a first-order transition is

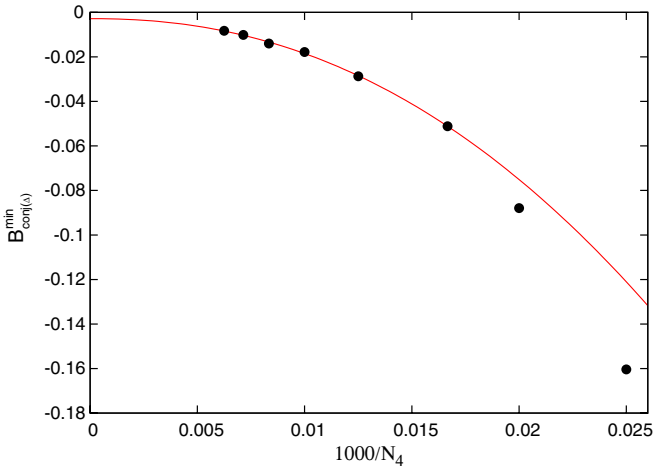

FIG. 3 (color online). Dependence of the minimum of the Binder cumulant $B_{\mathrm{conj}(\Delta)}$ on the (inverse) system size at the B-C transition. At a second-order transition, $B^{\min} \to 0$ in the infinite-volume limit. (Fit excludes the two points on the right.)

TABLE I. Measurements of $B_{\mathcal{O}}^{\min}(N_4 \to \infty)$ for various observables $\mathcal{O}$, where N_k denotes the number of k-dimensional (sub-) simplices in the triangulation.

Observable $\mathcal{O}$	$B_{\mathcal{O}}^{\min}(N_4 \to \infty)$
conj(Δ)	$-0.003(4)$
$N_4^{(4,1)}$	$-0.001(3)$
N_2	$-0.000\,000\,1(3)$
N_1	$-0.000\,003(7)$
N_0	$0.000\,0(3)$

clearly violated. (By contrast, for the A-C transition one finds $\tilde{\nu} \approx 1$ as will be reported elsewhere [22].)

Last, we have investigated how the minimum of the Binder cumulant (4) depends on the system size. Figure 3 shows $B_{\mathrm{conj}(\Delta)}^{\min}$ as a function of inverse system size (errors approximately equal to the dot radii). Inside the scaling region the minimum of the cumulant is expected to have a power-law behavior. To understand which data points lie inside the scaling region, we have again performed a sequence of fits by successively removing the points of lowest four-volume. This has led to the exclusion of the data points for $N_4 = 40k$ and $N_4 = 50k$ from the fit shown in Fig. 3.

Table I collects the extrapolations $B_{\mathcal{O}}^{\min}(N_4 \to \infty)$ for several observables $\mathcal{O}$. As indicated earlier, it is always difficult to make a strong case for a second-order transition based on Binder cumulant measurements alone, because weak first-order transitions may show a convergence to a nonzero value close to zero. Nevertheless, in the case at hand all our measurements are mutually consistent and in excellent agreement with the limiting value 0, further corroborating our claim of the second-order nature of the transition.

Discussion.—We have succeeded in our goal of determining the order of the B-C transition in CDT quantum gravity by applying two distinct methods, namely, measuring the shift exponent and analyzing Binder cumulants. The measured shift exponent $\tilde{\nu} = 2.51(3)$ represents a strong violation of the prediction $\tilde{\nu} = 1$ for a first-order transition. Also the results of the Binder cumulant analysis are clearly and unambiguously consistent with the second-order nature of the transition.

From this we conclude that there is strong evidence that the B-C transition is of second order, making four-dimensional CDT quantum gravity the first known instance of a dynamically triangulated model (without matter coupling) in any signature and dimension which displays such a transition. This result is potentially very attractive. It opens the door to studying critical phenomena in CDT and defining a continuum limit where the lattice spacing (the UV cutoff) is taken to zero, just as one does in standard lattice quantum field theories with nondynamical geometry.

S. J. thanks Professor G. T. Barkema for fruitful discussions and valuable advice on the numerical aspects of this work. J. A. thanks the ITP, Utrecht for hospitality. R. L. acknowledges support by the Netherlands Organisation for Scientific Research (NWO) under their VICI program. The contributions by S. J. and R. L. are part of the research programme of the Foundation for Fundamental Research on Matter (FOM), financially supported by NWO.

*ambjorn@nbi.dk
†s.jordan@uu.nl, r.loll@uu.nl
‡jurkiewicz@th.if.uj.edu.pl

[1] J. Ambjørn and S. Varsted, Nucl. Phys. **B373**, 557 (1992); Phys. Lett. B **266**, 285 (1991); J. Ambjørn, D. V. Boulatov, A. Krzywicki, and S. Varsted, Phys. Lett. B **276**, 432 (1992).
[2] M. E. Agishtein and A. A. Migdal, Mod. Phys. Lett. A **6**, 1863 (1991).
[3] D. V. Boulatov and A. Krzywicki, Mod. Phys. Lett. A **6**, 3005 (1991).
[4] J. Ambjørn and J. Jurkiewicz, Phys. Lett. B **278**, 42 (1992).
[5] M. E. Agishtein and A. A. Migdal, Mod. Phys. Lett. A **7**, 1039 (1992).
[6] M. Reuter and F. Saueressig, in *Geometric and Topological Methods for Quantum Field Theory*, edited by Hernan Ocampo (Cambridge University Press, Cambridge, U.K., 2010), pp. 288–329; M. Niedermaier and M. Reuter, Living Rev. Relativity **9**, 5 (2006).
[7] J. Ambjørn and J. Jurkiewicz, Nucl. Phys. **B451**, 643 (1995).
[8] B. V. de Bakker and J. Smit, Nucl. Phys. **B439**, 239 (1995); S. Catterall, J. B.Kogut, and R. Renken, Phys. Lett. B **328**, 277 (1994); H. S. Egawa, T. Hotta, T. Izubuchi, N. Tsuda, and T. Yukawa, Prog. Theor. Phys. **97**, 539 (1997).
[9] P. Bialas, Z. Burda, A. Krzywicki, and B. Petersson, Nucl. Phys. **B472**, 293 (1996).
[10] B. V. de Bakker, Phys. Lett. B **389**, 238 (1996).
[11] J. Ambjørn, J. Jurkiewicz, and R. Loll, Phys. Rev. Lett. **93**, 131301 (2004).
[12] P. Hořava, Phys. Rev. D **79**, 084008 (2009).
[13] J. Ambjørn, A. Görlich, S. Jordan, J. Jurkiewicz, and R. Loll, Phys. Lett. B **690**, 413 (2010).
[14] J. Ambjørn, J. Jurkiewicz, and R. Loll, Phys. Rev. D **72**, 064014 (2005).
[15] J. Ambjørn, J. Jurkiewicz, and R. Loll, Phys. Rev. Lett. **85**, 924 (2000); Nucl. Phys. **B610**, 347 (2001).
[16] J. Ambjørn, A. Görlich, J. Jurkiewicz, and R. Loll, Phys. Rev. Lett. **100**, 091304 (2008).
[17] J. Ambjørn, A. Görlich, J. Jurkiewicz, and R. Loll, Phys. Rev. D **78**, 063544 (2008).
[18] J. Ambjørn, A. Görlich, J. Jurkiewicz, and R. Loll, arXiv:1007.2560; J. Ambjørn, J. Jurkiewicz, and R. Loll, Contemp. Phys. **47**, 103 (2006); *Approaches to Quantum Gravity*, edited by D. Oriti (Cambridge University Press, Cambridge, U.K., 2009) pp. 341–359.
[19] T. Regge, Nuovo Cimento **19**, 558 (1961).
[20] J. Ambjørn, J. Jurkiewicz, and R. Loll, Phys. Lett. B **607**, 205 (2005).

[21] J. Ambjørn, A. Görlich, J. Jurkiewicz, R. Loll, J. Gizbert-Studnicki, and T. Trzesniewski, Nucl. Phys. **B849**, 144 (2011).

[22] J. Ambjørn, S. Jordan, J Jurkiewicz, and R. Loll (to be published).

[23] M. E. J. Newman and G. T. Barkema, *Monte Carlo Methods in Statistical Physics* (Oxford University Press, Oxford, 1999).

[24] H. Meyer-Ortmanns, Rev. Mod. Phys. **68**, 473 (1996).